



MDR1 and BCRP Transporter-Mediated Drug-Drug Interaction between Rilpivirine and Abacavir and Effect on Intestinal Absorption

Josef Reznicek, Martina Ceckova, Zuzana Ptackova, Ondrej Martinec, Lenka Tupova, Lukas Cervený,  Frantisek Staud

Charles University, Faculty of Pharmacy in Hradec Kralove, Department of Pharmacology and Toxicology, Hradec Kralove, Czech Republic

ABSTRACT Rilpivirine (TMC278) is a highly potent nonnucleoside reverse transcriptase inhibitor (NNRTI) representing an effective component of combination antiretroviral therapy (cART) in the treatment of HIV-positive patients. Many antiretroviral drugs commonly used in cART are substrates of ATP-binding cassette (ABC) and/or solute carrier (SLC) drug transporters and, therefore, are prone to pharmacokinetic drug-drug interactions (DDIs). The aim of our study was to evaluate rilpivirine interactions with abacavir and lamivudine on selected ABC and SLC transporters *in vitro* and assess its importance for pharmacokinetics *in vivo*. Using accumulation assays in MDCK cells overexpressing selected ABC or SLC drug transporters, we revealed rilpivirine as a potent inhibitor of MDR1 and BCRP, but not MRP2, OCT1, OCT2, or MATE1. Subsequent transport experiments across monolayers of MDCKII-MDR1, MDCKII-BCRP, and Caco-2 cells demonstrated that rilpivirine inhibits MDR1- and BCRP-mediated efflux of abacavir and increases its transmembrane transport. *In vivo* experiments in male Wistar rats confirmed inhibition of MDR1/BCRP in the small intestine, leading to a significant increase in oral bioavailability of abacavir. In conclusion, rilpivirine inhibits MDR1 and BCRP transporters and may affect pharmacokinetic behavior of concomitantly administered substrates of these transporters, such as abacavir.

KEYWORDS drug transporter, rilpivirine, abacavir, oral bioavailability, pharmacokinetics, drug-drug interactions, ABC transporters

Rilpivirine is a novel nonnucleoside reverse transcriptase inhibitor (NNRTI) approved by the FDA (in 2011) and the European Medicines Agency (EMA; in 2012) (1, 2) for treatment of antiretroviral therapy-naïve patients (3, 4). In addition, rilpivirine shows fewer adverse effects than efavirenz and represents an important component of combination antiretroviral therapy (cART), particularly in the treatment of HIV-1-infected patients with viral loads of less than 100,000 copies/ml (5).

Many antiretroviral drugs commonly used in cART are substrates or inhibitors of ABC (ATP-dependent) and/or SLC (solute carrier) drug transporters (6–9). Their coadministration with other compounds interacting with these transporters can lead to pharmacokinetic drug-drug interactions (DDIs) and to altered plasma and tissue concentrations of the target drug.

P-glycoprotein (ABCB1/MDR1) (10, 11), breast cancer resistance protein (ABCG2/BCRP) (12), and multidrug resistance-associated protein 2 (ABCC2/MRP2) (13) are well-described members of ATP-binding cassette (ABC) drug transporters that are functionally expressed in the small intestine, blood-tissue barriers, and excretory organs (14–17). Together with organic cation transporters (OCTs; SLC22A) of the SLC super-

Received 20 April 2017 Returned for modification 12 June 2017 Accepted 24 June 2017

Accepted manuscript posted online 10 July 2017

Citation Reznicek J, Ceckova M, Ptackova Z, Martinec O, Tupova L, Cervený L, Staud F. 2017. MDR1 and BCRP transporter-mediated drug-drug interaction between rilpivirine and abacavir and effect on intestinal absorption. *Antimicrob Agents Chemother* 61:e00837-17. <https://doi.org/10.1128/AAC.00837-17>.

Copyright © 2017 American Society for Microbiology. All Rights Reserved.

Address correspondence to Frantisek Staud, frantisek.staud@faf.cuni.cz.

family, they largely influence intestinal absorption and diminish distribution of drugs into sensitive body tissues (14, 15, 17, 18). By cooperation with organic cation transporters and multidrug and toxin extrusion proteins (MATEs; *SLC47A*), ABC transporters also promote the renal and hepatic excretion of drugs from blood to urine and bile, respectively (14, 16, 19–21). The role of these transporters as the major determinants of pharmacokinetics, drug safety, and efficacy and their potential to cause DDIs is, therefore, of clinical and regulatory concern (22–26).

A current literature search indicates rilpivirine is an inhibitor but not substrate of various ABC and OCT transporters (27, 28); however, its potential for DDIs has not been fully elucidated to date. While a small early-onset increase in creatinine levels in the group of rilpivirine-treated patients has been associated with OCT inhibition in the proximal renal tubule (29), other studies conclude that rilpivirine-mediated inhibition of transporters is not expected to have a systemic relevance (1, 27, 28). The EMA, however, suggests that even though rilpivirine did not show any effect on the pharmacokinetics of digoxin, a recognized MDR1 substrate, it might increase the exposure to other MDR1 substrates whose absorption is more sensitive to intestinal MDR1 inhibition (1). We further hypothesize that BCRP inhibition contributes to the DDIs of rilpivirine, particularly with dual MDR1/BCRP substrates, such as tenofovir disoproxil fumarate (TDF) (1).

Besides the traditional one-pill coadministration of rilpivirine with TDF and emtricitabine, a new cost-effective, safe, and clinically efficient combination of rilpivirine with two other NRTIs, abacavir and lamivudine, has been suggested (30–32). Both abacavir and lamivudine are recognized substrates of various membrane transporters (7, 33, 34). While abacavir is transported by MDR1 and BCRP (7), lamivudine pharmacokinetics are affected mainly by OCT and MATE transporters (33, 34). Therefore, we hypothesize that the inhibition of ABC transporters by rilpivirine results in interaction with abacavir, particularly on the level of intestinal absorption. In addition, inhibition of MATE1 and/or OCTs could affect active renal excretion of lamivudine.

In the present study, we employed *in vitro* models of transporter-overexpressing MDCKII cells and Caco-2 monolayers along with an *in vivo* pharmacokinetic assay in male Wistar rats to (i) verify the inhibitory effect of rilpivirine to MDR1, BCRP, MRP2, OCT1, OCT2, or MATE1 transporters and to (ii) investigate possible ABC and/or SLC transporter-mediated interactions between rilpivirine and abacavir or lamivudine.

RESULTS

Inhibitory effect of rilpivirine on MDR1, BCRP, and MRP2. Using the accumulation and efflux assays with standardly used fluorescent substrates Hoechst 33342, rhodamine 123, and/or calcein AM, we tested inhibitory potency of rilpivirine toward MDR1, BCRP, and MRP2. Rilpivirine in 1 and 10 μM concentrations significantly inhibited efflux of Hoechst 33342 (80 μM) from MDCK-MDR1 but not from MDCK-PAR cell lines (Fig. 1A and B). We also observed inhibition of rhodamine 123 (10 μM) efflux from MDCK-MDR1 but not from MDCK parental cells with 10 μM (but not 1 μM) rilpivirine (Fig. 1C and D). Efflux of Hoechst 33342 from MDCK-BCRP but not from MDCK parental cells was inhibited by 1 and 10 μM rilpivirine (Fig. 1E and F). Nevertheless, rilpivirine at up to 10 μM concentration did not inhibit efflux of calcein from MDCK-MRP2 or MDCK parental cells (Fig. 1G and H). These results indicate inhibitory potency of rilpivirine toward MDR1 and BCRP but not MRP2. The inhibitory effect of rilpivirine to MDR1 and BCRP did not, however, reach the effect of control inhibitor LY335979 (1 μM) or Ko143 (2.5 μM), even when applied at the highest (10 μM) concentration.

Inhibitory effect of rilpivirine on OCT1, OCT2, or MATE1. Employing accumulation experiments with ASP⁺ (1 μM), a common fluorescent substrate of OCT1, OCT2, and MATE1, we studied the inhibitory effect of rilpivirine on these transporters. However, in contrast to a model inhibitor, mitoxantrone (MTX), rilpivirine did not affect accumulation of ASP⁺ in any of the MDCK-OCT1, MDCK-OCT2, MDCK-MATE1, or MDCK-Co cells when applied in a concentration range from 0.001 to 10 μM (Fig. 2). These results suggest no significant inhibitory potency of rilpivirine toward OCT1, OCT2, or MATE1 transporter.

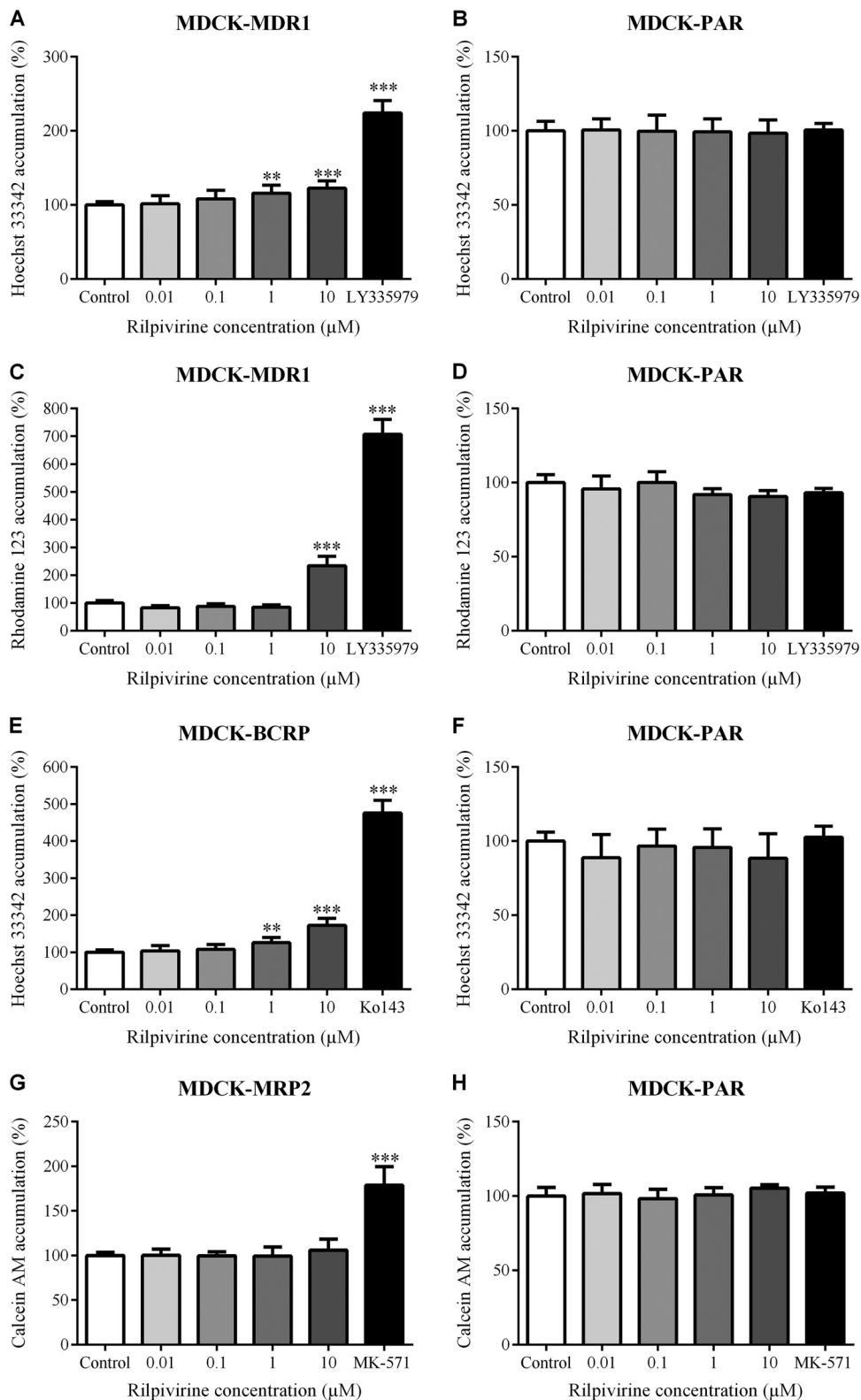


FIG 1 Inhibitory effect of rilpivirine on efflux of Hoechst 33342 (80 μM) from MDCK-MDR1 (A), MDCK-BCRP (E), and MDCK-PAR (B and F) cell lines; efflux of rhodamine 123 (10 μM) from MDCK-MDR1 (C) and MDCK-PAR (D) cells; and efflux of calcein AM (0.25 μM) from MDCK-MRP2 (G) and MDCK-PAR (H) cell lines. LY335979 (1 μM), Ko143 (2.5 μM), and MK-571 (50 μM), the model inhibitors of MDR1, BCRP, and MRP2, respectively, were used as positive controls. Data are shown as mean values ± SD from at least three experiments performed in triplicate. Statistical significance was analyzed by one-way ANOVA followed by Bonferroni's test. **, $P \leq 0.01$; ***, $P \leq 0.001$.

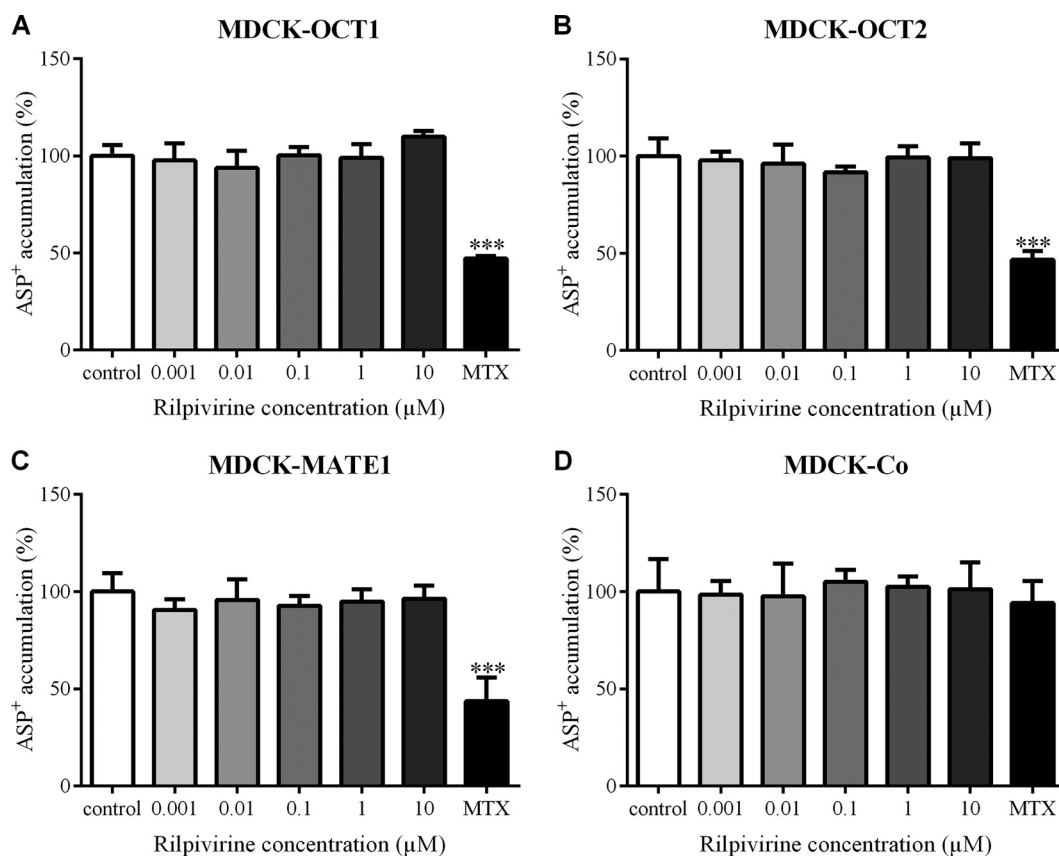


FIG 2 Effect of rilpivirine on accumulation of ASP⁺ (1 μM) in MDCK-OCT1 (A), MDCK-OCT2 (B), MDCK-MATE1 (C), and MDCK-Co (D) cell lines. Mitoxantrone (MTX), a model inhibitor of OCT1, OCT2, and MATE1, was used as a positive control at a concentration of 2 μM. Data are shown as mean values ± SD from four experiments performed in triplicate. Statistical significance was analyzed by one-way ANOVA followed by Bonferroni's test. ***, $P \leq 0.001$.

Inhibitory effect of rilpivirine on MDR1- and BCRP-mediated transport of abacavir across MDCK cell monolayers. Employing the concentration equilibrium method, we further evaluated the inhibitory effect of rilpivirine on transcellular transport of 300 nM abacavir across monolayers of MDCK-MDR1 and MDCK-BCRP cells. Expression of genes encoding human MDR1 (ABCB1) and BCRP (ABCG2) in respective MDCK cell lines used for transport experiments was verified and quantified previously (35, 36). Significant asymmetry (***, $P \leq 0.001$) in abacavir concentrations between the apical and basolateral compartments after 6 h of abacavir incubation was observed in MDCK-MDR1 as well as in the MDCK-BCRP cells, reaching the respective concentration ratios (r_e) of 2.09 and 2.01 (Fig. 3A and B). When 0.1 or 1 μM rilpivirine was added to the MDCK-MDR1 monolayers, the asymmetry between abacavir concentrations in the apical and basolateral compartments was still significant (***, $P \leq 0.001$), but the relevant concentration ratios decreased to an r_e of 1.87 or 1.27, respectively. Rilpivirine administered at a concentration of 10 μM eliminated this asymmetry as potently as the control inhibitor LY335979 (r_e of 1.01 and 0.99, respectively).

Concentration-dependent inhibitory effect of rilpivirine on the transcellular transport of abacavir also was observed in the MDCK-BCRP monolayers, showing complete inhibition at a concentration of 0.5 μM (Fig. 3B). Our results thus demonstrate the inhibitory effect of rilpivirine on the MDR1- and BCRP-mediated abacavir efflux, showing transporter-mediated interaction between these two antiretrovirals *in vitro*.

Effect of rilpivirine on bidirectional permeation of abacavir across Caco-2 monolayers. To study the effect of rilpivirine on the permeation of abacavir under more physiologically relevant conditions, we employed bidirectional transport studies across monolayers of Caco-2 cells, a widely accepted model of intestinal drug absorp-

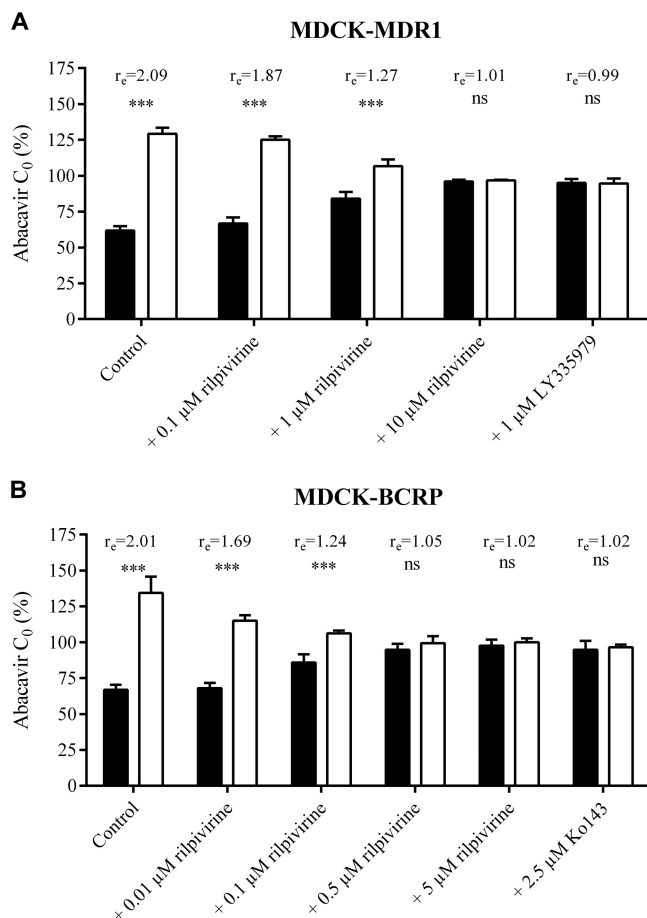


FIG 3 Concentration equilibrium assay of [³H]abacavir (300 nM) in MDCK-MDR1 (A) and MDCK-BCRP (B) cells. The percentage of initial concentration (C₀) of abacavir obtained in the basolateral (black columns) or apical compartment (white columns) after 6 h of incubation with or without rilpivirine is shown. LY335979 (1 μM) or Ko143 (2.5 μM) was used as a positive control. The ratio (r_c) between concentrations in the apical and basolateral compartments measured at the end of the experiment is shown. Data are shown as mean values ± SD from three experiments performed in duplicate. Statistical significance was analyzed by Student's *t* test. ***, *P* ≤ 0.001; ns, not significant.

tion (22, 24, 37). Using quantitative real-time reverse transcription-PCR (qRT-PCR), we first quantified expression of genes encoding human MDR1 (*ABCB1*) and BCRP (*ABCG2*) in our Caco-2 cell culture, which revealed the same numbers of *ABCB1* transcripts ($177 \times 10^4 \pm 55.4 \times 10^4$) but almost ten-times-higher levels of *ABCG2* ($24.8 \times 10^4 \pm 1.37 \times 10^4$) (data shown are means ± standard deviations from three experiments performed in triplicate) compared to another study on Caco-2 cells obtained from the American Type Culture Collection (38). The abacavir (300 nM) basolateral-to-apical (B-to-A) apparent permeability coefficient (*P*_{app}) was significantly (***, *P* ≤ 0.001) increased compared to apical-to-basolateral (A-to-B) *P*_{app}, with an efflux ratio (ER) of 2.40 (Fig. 4). Comparison of abacavir permeability in both basolateral-to-apical and apical-to-basolateral directions in the presence of 10 μM rilpivirine showed complete blockage of abacavir efflux transport, with an ER of 0.92. The effect of rilpivirine on abacavir permeation was similar to the effect of GF120918 (2 μM). Our results indicate that 10 μM rilpivirine increased apical-to-basolateral abacavir permeation and decreased secretory transport in Caco-2 cells.

Influence of rilpivirine on abacavir intestinal absorption *in vivo*. Employing pharmacokinetic experiments with male Wistar rats, we studied the effect of rilpivirine on intestinal absorption of abacavir. Intraduodenally administered rilpivirine (300 μM) significantly increased (*, *P* ≤ 0.05) the area under the curve (AUC) of coadministered radiolabeled abacavir (300 μM) (Fig. 5).

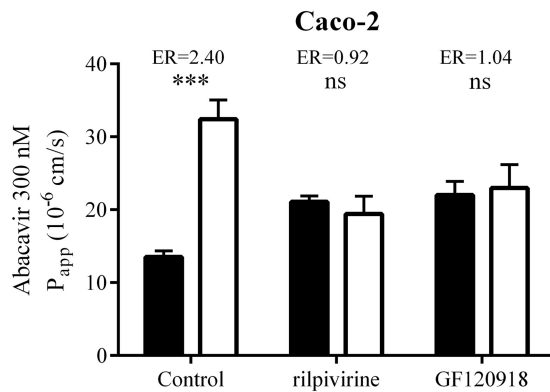


FIG 4 Effect of 10 μ M rilpivirine and 2 μ M GF120918 on bidirectional permeation of 300 nM abacavir through Caco-2 monolayers. Apical-to-basolateral (A-to-B) P_{app} (black columns) or basolateral-to-apical (B-to-A) P_{app} (white columns) after 1 h of incubation with or without rilpivirine or GF120918 is shown. The efflux ratio (ER) was defined as the B-to-A P_{app} divided by the A-to-B P_{app} . Data are shown as mean values \pm SD from three experiments performed in duplicate. Statistical significance was analyzed by Student's *t* test. ***, $P \leq 0.001$; ns, not significant.

DISCUSSION

Administration of two or more drugs, which is a typical scenario in the treatment of HIV-positive patients, often bears the risk of pharmacokinetic drug-drug interactions (DDIs) (39). Drug transporters, largely expressed in many human tissues, may be involved in development of such DDIs (6, 40–43). Therefore, in this study, we aimed to (i) assess the inhibitory potential of an NNRTI antiretroviral drug, rilpivirine, to the selected ABC efflux transporters (MDR1, BCRP, and MRP2) and SLC transporters (OCT1, OCT2, and MATE1) and (ii) to evaluate the potential of rilpivirine to interact with abacavir and lamivudine. While abacavir is a confirmed substrate of MDR1 and BCRP, lamivudine has recently been found to be transported by OCTs and MATE1 transporters (7, 33, 34). Therefore, the risk of transporter-mediated DDIs between rilpivirine, abacavir, and/or lamivudine might be relatively high.

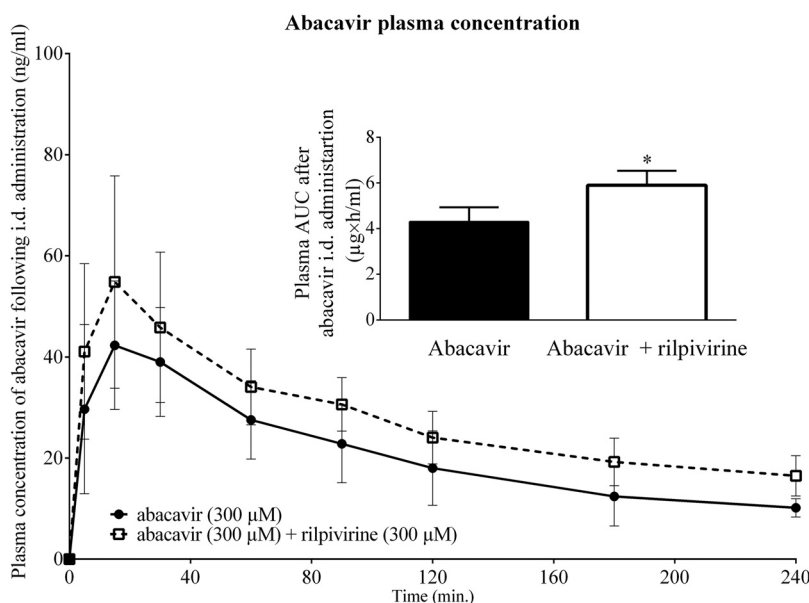


FIG 5 Influence of rilpivirine (300 μ M) on plasma concentration of abacavir (300 μ M) after i.d. administration. Data are shown as means \pm SD ($n = 6$). Statistical significance was analyzed by unpaired *t* test. *, $P \leq 0.05$. The rilpivirine $AUC_{0-240 \text{ min}}$ was calculated using the trapezoid rule, where the formula $\Delta X \times (Y1 + Y2)/2$ was used repeatedly by GraphPad Prism 6.0 software (GraphPad Software, Inc., San Diego, CA, USA).

Weiss and Haefeli (27) have recently reported inhibitory properties of rilpivirine to MDR1 and BCRP, showing inhibition of calcein acetoxymethyl ester and pheophorbide A accumulation in L-MDR1 and MDCK-BCRP cells, respectively. However, several binding sites on the MDR1 molecule have been proposed (44, 45), making the issue of MDR1-mediated DDIs more intricate. Therefore, two model MDR1 substrates, Hoechst 33342 and rhodamine 123, specific for two different binding sites, were employed in our study. A significant increase in the accumulation of Hoechst 33342 in MDCK-MDR1 and MDCK-BCRP (but not in MDCK-PAR) was observed when rilpivirine was added at concentrations of $\geq 1 \mu\text{M}$. Rilpivirine ($10 \mu\text{M}$) also increased the uptake of rhodamine 123 in MDCK-MDR1 (but not MDCK-PAR) cells. Our data thereby show the ability of rilpivirine to interact with distinct sites of MDR1 transport protein, suggesting high DDI potential. On the other hand, accumulation of calcein in MDCK-MRP2 cells was not influenced by rilpivirine, suggesting no inhibitory potency of rilpivirine toward this transporter up to a $10 \mu\text{M}$ concentration.

Regarding SLC transporters, we are the first to show the lack of interaction of rilpivirine with MATE1 transporter. In contrast, Moss et al. reported a negligible inhibitory effect of rilpivirine on tetraethyl ammonium uptake in OCT1-expressing KCL22 cells and a weak inhibition (up to $\sim 45\%$ at $10 \mu\text{M}$ rilpivirine) of metformin uptake into OCT2-expressing *X. laevis* oocytes (28). In our study, however, we failed to confirm Moss's results, as we could not observe any inhibitory effect of rilpivirine on OCT1- or OCT2-mediated uptake of ASP^+ in MDCK-OCT1 or MDCK-OCT2 cells. This discrepancy might be explained by different cellular models and substrates used in our and Moss et al.'s study. Moreover, Moss et al. tested rilpivirine at significantly higher concentrations, which could not be achieved in our experiments due to limited solubility of the drug (0.0116 mg/ml). Nevertheless, concentrations of rilpivirine inhibitory to OCT1 and OCT2 in the abovementioned study are more than 12 and 70 times higher, respectively, than the average steady-state plasma rilpivirine concentration ($0.43 \mu\text{mol/liter}$) achieved by regular administration of the standard 25-mg/day doses (46). Since rilpivirine is extensively metabolized by cytochrome P450 (CYP) 3A4 and strongly bound to plasma proteins (99.7%), its free plasma concentrations at steady state approach 1.2 nM (27, 47, 48). Therefore, it seems unlikely that rilpivirine concentrations achieved in plasma will be sufficient for inhibition of OCTs *in vivo* and for development of clinically relevant systemic DDIs. Consistent with the above-described data, inhibition of renal OCTs in rilpivirine therapy causes only mild early-onset increases in creatinine plasma levels, which is not considered clinically relevant (29). Therefore, we do not expect any clinically relevant transporter-mediated DDIs of rilpivirine combined with lamivudine, the OCTs, and MATE substrate.

In subsequent studies, we focused on MDR1/BCRP-based DDIs between rilpivirine and abacavir. When investigating transport of abacavir across monolayers of MDCK cells, we observed inhibition of the MDR1- and BCRP-mediated efflux of abacavir in the presence of rilpivirine, reaching complete inhibition at concentrations exceeding $10 \mu\text{M}$ and $0.5 \mu\text{M}$, respectively. As mentioned above, lower plasma concentrations of rilpivirine are achieved during therapy, questioning the significance of these *in vitro* results for the systemic DDIs *in vivo*. However, after oral administration, local rilpivirine concentrations in the gastrointestinal tract may be sufficient to inhibit intestinal transporters. Considering high expression of MDR1 and BCRP in the small intestine and their role in limiting drug absorption (14), we hypothesized that rilpivirine increases abacavir bioavailability after oral administration. To investigate this issue on an *in vitro* level, we employed Caco-2 cells, a widely used model of intestinal barrier (22). Transport assays across monolayers of Caco-2 cells indicated a significant effect of rilpivirine on the transcellular permeation of abacavir, suggesting transporter-mediated DDIs between these two antiretrovirals.

The International Transporter Consortium recommends the performance of *in vivo* studies if the $[I]_2/IC_{50}$ (or K_i) ratio is ≥ 10 , where IC_{50} is the 50% inhibitory concentration and $[I]_2$ is the theoretical maximal gastrointestinal drug concentration after oral administration, calculated as the highest clinical dose (in milligrams) in a volume of 250

ml (24, 37). Considering the estimated half-maximal inhibitory concentrations observed in our *in vitro* transport assays and the recommended clinical dose of 25 mg/day, the abovementioned ratio exceeds a value of 10 for both MDR1 and BCRP transporters. Therefore, we subsequently performed *in vivo* absorption experiments in Wistar rats to study the effect of rilpivirine on abacavir oral bioavailability. Abacavir was administered at a concentration ensuring reliable analysis of the drug in plasma; rilpivirine was used at an equimolar concentration corresponding to that achieved in clinical settings. Using this *in vivo* setup, we show significant increase (by 37%) in the bioavailability of intraduodenally administered abacavir when coadministered with rilpivirine. Based on our results, we suggest that this increase is caused by inhibition of intestinal MDR1 and BCRP caused by rilpivirine. If confirmed in human, we assume that this DDI can be exploited in clinical settings, leading to a decreased abacavir dose in oral cART.

In conclusion, we demonstrate rilpivirine as an inhibitor of BCRP and MDR1. On the other hand, rilpivirine inhibitory potency was observed neither toward OCT1 or OCT2 uptake carriers nor toward MRP2 or MATE1 efflux transporters up to a 10 μ M concentration. We further revealed transporter-mediated DDIs between rilpivirine and abacavir *in vitro* and demonstrated the relevance of this interaction for abacavir intestinal absorption *in vivo*. Further studies are needed to evaluate our findings in clinical settings and to reveal the potential of rilpivirine to increase bioavailability of other MDR1 and/or BCRP substrates.

MATERIALS AND METHODS

Chemicals and reagents. Radiolabeled abacavir ($[^3\text{H}]$ abacavir; 0.1 Ci/mmol) was purchased from Moravek Biochemicals, CA, USA. Dulbecco's modified Eagle's medium (DMEM), Opti-MEM, fetal bovine serum (FBS), nonessential amino acids solution (NEAA), penicillin-streptomycin solution, and scintillation cocktail were purchased from Sigma-Aldrich (St. Louis, MO, USA). Solvable was purchased from PerkinElmer (Waltham, MA, USA). Rilpivirine was obtained from the NIH AIDS Reagent Program and from Toronto Research Chemicals (Toronto, Canada). The dual ABCG2 and ABCB1 inhibitor, GF120918 (Elacridar), was kindly provided by GlaxoSmithKline (Greenford, United Kingdom). Pentobarbital (Nembutal) was obtained from Abbott Laboratories (Abbott Park, IL, USA). Other chemicals, including MDR1 inhibitor LY-335979 (Zosuquidar) and BCRP inhibitor Ko143, were of analytical grade and obtained from Sigma-Aldrich.

Cell cultures. The MDCK parental cell line and MDCK cells stably transduced for expression of human transporter MDR1, BCRP, or MRP2 (MDCK-PAR, MDCK-MDR1, MDCK-BCRP, and MDCK-MRP2) were provided by Alfred Schinkel (The Netherlands Cancer Institute, Amsterdam, The Netherlands). All of the MDCK cell lines were cultured in DMEM complete high-glucose medium with L-glutamine supplemented with 10% FBS. Transfected MDCKII cell lines stably expressing human OCT1, OCT2, and/or MATE1 (MDCK-OCT1, MDCK-OCT2, and MDCK-MATE1 cells), as well as the vector control cell line MDCK-Co, were provided by Martin F. Fromm (Institute of Experimental and Clinical Pharmacology and Toxicology, Friedrich-Alexander-Universität Erlangen-Nürnberg, Erlangen, Germany) and cultured in MEM supplemented with 10% FBS. The Caco-2 cell line was obtained from the European Collection of Authenticated Cell Cultures (ECACC) and cultured in DMEM complete high-glucose medium with L-glutamine, supplemented with 10% FBS and 1% NEAA. Cell lines were routinely cultivated in antibiotic-free medium and periodically tested for mycoplasma contamination. Stable expression of all transporters was verified by qRT-PCR and uptake assays with corresponding fluorescence substrates. Cells from passages 10 to 25 were used in all *in vitro* studies.

Animals. Wistar male rats (240 to 280 g) were purchased from MediTox Ltd. (Konarovice, Czech Republic) and maintained under 12-h day/12-h night standard conditions with water and pellets *ad libitum*. Fasted rats were anesthetized by 40 mg/kg of body weight pentobarbital (Abbott Laboratories, Abbott Park, IL) administered into the tail vein. All experiments were approved by the Ethical Committee of the Faculty of Pharmacy in Hradec Kralove (Charles University, Prague, Czech Republic) and were carried out in accordance with the *Guide for the Care and Use of Laboratory Animals* (49) and the *European Convention for the Protection of Vertebrate Animals Used for Experimental and Other Scientific Purposes* (50).

qRT-PCR quantification of ABCB1 and ABCG2 transcripts in Caco-2 cells. To evaluate and compare ABCB1 and ABCG2 transcript levels in the Caco-2 cell line used in this study, we used qRT-PCR analysis. Total RNA was isolated from the cell line grown in culture flasks using TRI Reagent (Molecular Research Centre, Cincinnati, OH, USA) according to the manufacturer's instructions. The absorbance of isolated RNA was measured at 260 nm and 280 nm using a NanoDrop spectrometer (Thermo Fisher Scientific, Waltham, MA, USA). To check the concentration and purity, cDNA was prepared from 1- μ g portions of the extracted total RNA with Moloney murine leukemia virus (MMLV) transcriptase using oligo(dT)₁₈VN nucleotides and porcine RNase inhibitor (Tetro cDNA synthesis kit; Bioline, London, United Kingdom). We then amplified cDNA (from 40 ng of transcribed RNA) by real-time PCR using a QuantStudio 6 Flex real-time PCR system (Thermo Fisher Scientific, Waltham, MA, USA) and a master mix containing 26 probes (Generi Biotech, Hradec Kralove, Czech Republic) in predesigned PCR assays for ABCB1 or ABCG2 (hABCB1_Q2 or hABCG2_Q2; Generi Biotech, Hradec Kralove, Czech Republic). For

absolute quantification, PCR plasmids (Generi Biotech, Hradec Kralove, Czech Republic) hosting sub-cloned PCR products of ABCB1 or ABCG2 were used as PCR standards. Each sample and standard was amplified in triplicate by incubation at 95°C for 3 min, followed by 40 cycles of 95°C for 10 s and 60°C for 20 s. Standard curves were generated by preparing and amplifying seven decimal dilutions of the ABCB1 or ABCG2 PCR plasmid; the number of copies ranged from 1.10^7 to 1.10^1 copies/20-ml reaction. The resulting real-time amplification curves were analyzed and threshold cycle (C_T) values subtracted using QuantStudio 6 Flex software (Thermo Fisher Scientific, Waltham, MA, USA). Excel software (Microsoft, Seattle, WA, USA) was used for all other calculations, and the absolute number of cDNA copies in each sample was calculated from the generated calibration curves.

In vitro experiments. (i) Hoechst 33342 and rhodamine 123 accumulation assay. MDCK cells expressing MDR1 or BCRP transporters or parental cells were seeded on 96-well plates at a density of 25×10^3 cells per well and cultivated in DMEM supplemented with 10% FBS. Forty-eight hours after seeding, accumulation experiments with Hoechst 33342, a common fluorescence substrate of MDR1 and BCRP, or rhodamine 123, another model fluorescence substrate of MDR1, were performed. Medium was aspirated and cells were washed with prewarmed phosphate-buffered saline (PBS). Opti-MEM with or without rilpivirine was added for 30 min. After this time, Hoechst 33342 (final concentration, 80 μ M) or rhodamine 123 (final concentration, 10 μ M) in Opti-MEM was added. After 30 min, cells were washed thrice with ice-cold PBS and fluorescence was measured at 350 nm for excitation and 465 nm for emission or at 485 nm for excitation and 535 nm for emission for Hoechst 33342 or rhodamine 123, respectively.

(ii) Calcein AM efflux assay. MDCK cells expressing MRP2 transporter or parental cells were seeded on 96-well plates at a density of 25×10^3 cells per well and cultivated in DMEM supplemented with 10% FBS. Forty-eight hours after seeding, accumulation experiments with calcein AM, which is extracellularly metabolized into calcein, a fluorescence substrate of MRP2, were performed. Medium was aspirated and cells were washed with prewarmed PBS. A solution of calcein AM in Opti-MEM was added for 15 min of preincubation. After this time, cells were washed with prewarmed PBS, and Opti-MEM with or without rilpivirine was added for 60 min. This efflux phase was stopped by aspiration of the media and washing the cells thrice with ice-cold PBS. Fluorescence was measured at 496 nm for excitation and 516 nm for emission.

(iii) ASP⁺ uptake assay. Single OCT1-, OCT2-, and MATE1-transfected MDCK cells and MDCK control cells were seeded on a 96-well plate at a density of 45×10^3 cells per well and cultivated in standard cultivation medium (MEM plus 10% FBS). Twenty-four hours after seeding, uptake experiments with ASP⁺, a common fluorescence substrate of OCT1, OCT2, and MATE1, were performed. Cells were washed twice with 100 μ l prewarmed Hanks' balanced salt solution (HBSS) buffer, pH 7.4. MATE1-expressing cells were preincubated with 100 μ l 20 mM NH₄Cl, pH 7.4, for 30 min. After washing the cells twice with 100 μ l prewarmed HBSS buffer, pH 8.0, ASP⁺ (1 μ M) with rilpivirine (0.01 to 10 μ M) was added for 20 min. The uptake was stopped by medium removal and three cell washes with ice-cold HBSS buffer (pH 7.4). Cellular fluorescence was subsequently measured at a wavelength of 485 nm for excitation and 585 nm for emission.

(iv) Concentration equilibrium transport assay in MDCK cells. Transport assays employing MDR1- or BCRP-expressing MDCK cells were performed on microporous polycarbonate membrane filters (3.0- μ m pore size, 24-mm diameter; Transwell 3414; Costar, Corning, NY) as described previously (7, 8). The cells were seeded at a density of 1×10^6 per insert and cultured for 4 days in standard cultivation medium, DMEM (Gibco) with 10% FBS, until reaching confluence, with daily replacement of cell culture medium. Thirty minutes before starting the experiment, cells were washed with prewarmed PBS and incubated with Opti-MEM with or without rilpivirine or control inhibitor. The transport assay was initiated by addition of [³H]abacavir (300 nM) with or without rilpivirine (or control inhibitor) to both apical and basal compartments, providing equal concentrations of the drug on both sides of the monolayer. For drug analysis, aliquots of 50 μ l were collected from both compartments at 2, 4, and 6 h, and radioactivity was measured by liquid scintillation counting (Tri-Carb 2900 TR; PerkinElmer). The equilibrium assay concentration ratio (r_e) was calculated as described earlier (7, 8) by dividing the concentration of [³H]abacavir in the apical compartment by the concentration in the basal compartment at the end (6 h) of the experiment. The integrity of the monolayer was verified by analyzing the leakage of fluorescein isothiocyanate-dextran (accepting up to 1% per hour).

(v) Bidirectional transport assay in Caco-2 monolayers. Transport assays employing the Caco-2 cell line were performed on collagen-coated microporous polycarbonate membrane filters (0.4- μ m pore size, 12-mm diameter; Transwell 3493; Costar, Corning, NY). Caco-2 cells were seeded at a density of 0.3×10^6 per insert, incubated at 37°C and 5% CO₂, and cultured for 21 days with replacement of cell culture medium supplemented with 1% penicillin-streptomycin every other day. The transepithelial electrical resistance (TEER) was measured using a Millicell ERS voltohmmeter (Millipore, Merck). After washing the monolayers with prewarmed PBS, the cells were preincubated with Opti-MEM with or without rilpivirine or control inhibitor. The transport assay was initiated by addition of [³H]abacavir with or without rilpivirine into the apical or basal compartment. The final activity of [³H]abacavir was 0.04 μ Ci/ml (300 nM), as dictated by the specific activity of radioisotopes required for analysis. Aliquots of 50 μ l were collected at 0.5, 1, 2, and 3 h from the acceptor compartment, and radioactivity was measured by liquid scintillation counting (Tri-Carb 2900 TR; PerkinElmer). Apparent permeability coefficients (P_{app}) were calculated using the equation $P_{app} = (dC/dt) \times V_r / (A \times C_0)$, where dC/dt is the change in concentration over time, as measured at 60 min (in micromolars per second), V_r is the volume of the receiver well (in cubed centimeters), A is the area of the cell monolayer (in square centimeters), and C_0 is the initial

concentration in the donor well (in micromolars) (51). The efflux ratio (ER) was defined as the B-to-A P_{app} divided by the A-to-B P_{app} .

In vivo pharmacokinetic experiments. In anesthetized rats, *vena jugularis*, bile duct, and urinary bladder were cannulated. Rilpivirine (300 μ M) or physiological saline (control group) were applied intraduodenally (i.d.) in an amount of 4 μ l per 5 g of animal weight, followed 20 min later by application of radiolabeled abacavir (300 μ M, 30 μ Ci/ml; 4 μ l per 5 g of animal weight) with or without rilpivirine (300 μ M). Rat blood was sampled from *vena jugularis* at the following time intervals: 5, 15, 30, 60, 90, 120, 180, and 240 min. The biological samples were dissolved in Solvable according to the manufacturer's protocol, and the radioactivity of the final samples was measured by liquid scintillation counting (Tri-Carb 2900 TR; PerkinElmer).

Statistical analyses. The statistical significance in transport assays using Caco-2 and MDCK cell lines was examined by unpaired Student's *t* test. When evaluating *in vivo* pharmacokinetic experiments and *in vitro* accumulation experiments, statistical significance was examined by one-way analysis of variance (ANOVA) followed by Bonferroni's test. The area under the curve from 0 to 240 min was calculated using the trapezoid rule, where the formula $\Delta X \times (Y1 + Y2)/2$ was used repeatedly. All data were analyzed and the result graphs prepared using GraphPad Prism 6.0 software (GraphPad Software, Inc., San Diego, CA, USA).

ACKNOWLEDGMENTS

The study was financially supported by the Czech Science Foundation (GACR 17-16169S) and the Grant Agency of the Charles University in Prague (SVV/2017/260 414). The funders had no role in study design, data collection and analysis, the decision to publish, or the preparation of the manuscript.

We thank Dana Souckova and Renata Exnarova for skillful assistance with the *in vivo* pharmacokinetic experiments.

REFERENCES

- European Medicines Agency. Edurant 25 mg film-coated tablets: summary of product characteristics. European Medicines Agency, London, United Kingdom. http://www.ema.europa.eu/docs/en_GB/document_library/EPAR_-_Product_Information/human/002264/WC500118874.pdf. Accessed 21 April 2016.
- Center for Drug Evaluation and Research. Clinical pharmacology and biopharmaceutics review(s), application number 202022Orig1s000. U.S. Food and Drug Administration, Washington, DC. http://www.accessdata.fda.gov/drugsatfda_docs/nda/2011/202022Orig1s000ClinPharmR.pdf. Accessed 21 April 2016.
- Azjin H, Tirry I, Vingerhoets J, de Bethune MP, Kraus G, Boven K, Jochmans D, Van Craenenbroeck E, Picchio G, Rimsky LT. 2010. TMC278, a next-generation nonnucleoside reverse transcriptase inhibitor (NNRTI), active against wild-type and NNRTI-resistant HIV-1. *Antimicrob Agents Chemother* 54:718–727. <https://doi.org/10.1128/AAC.00986-09>.
- Goebel F, Yakovlev A, Pozniak AL, Vinogradova E, Boogaerts G, Hoetelmans R, de Bethune MPP, Peeters M, Woodfall B. 2006. Short-term antiviral activity of TMC278—a novel NNRTI—in treatment-naïve HIV-1-infected subjects. *AIDS* 20:1721–1726. <https://doi.org/10.1097/01.aids.0000242818.65215.bd>.
- Panel on Antiretroviral Guidelines for Adults and Adolescents. 2016. Guidelines for the use of antiretroviral agents in HIV-1-infected adults and adolescents. Department of Health and Human Services, Washington, DC. <http://aidsinfo.nih.gov/contentfiles/lvguidelines/AdultandAdolescentGL.pdf>. Accessed 20 November 2016.
- Kis O, Robillard K, Chan GN, Bendayan R. 2010. The complexities of antiretroviral drug-drug interactions: role of ABC and SLC transporters. *Trends Pharmacol Sci* 31:22–35. <https://doi.org/10.1016/j.tips.2009.10.001>.
- Neumanova Z, Cerveny L, Greenwood SL, Ceckova M, Staud F. 2015. Effect of drug efflux transporters on placental transport of antiretroviral agent abacavir. *Reprod Toxicol* 57:176–182. <https://doi.org/10.1016/j.reprotox.2015.07.070>.
- Neumanova Z, Cerveny L, Ceckova M, Staud F. 2015. Role of ABCB1, ABCG2, ABCC2 and ABCC5 transporters in placental passage of zidovudine. *Biopharm Drug Dispos* 37:28–38. <https://doi.org/10.1002/bdd.1993>.
- Reznicek J, Ceckova M, Cerveny L, Muller F, Staud F. 2016. Emtricitabine is a substrate of MATE1 but not of OCT1, OCT2, P-gp, BCRP or MRP2 transporters. *Xenobiotica* 47:77–85. <https://doi.org/10.3109/00498254.2016.1158886>.
- Thiebaut F, Tsuruo T, Hamada H, Gottesman MM, Pastan I, Willingham MC. 1987. Cellular localization of the multidrug-resistance gene product P-glycoprotein in normal human tissues. *Proc Natl Acad Sci U S A* 84:7735–7738. <https://doi.org/10.1073/pnas.84.21.7735>.
- Roninson IB, Chin JE, Choi K, Gros P, Housman DE, Fojo A, Shen D, Gottesman MM, Pastan I. 1986. Isolation of human Mdr-DNA sequences amplified in multidrug-resistant Kb carcinoma cells. *Proc Natl Acad Sci U S A* 83:4538–4542. <https://doi.org/10.1073/pnas.83.12.4538>.
- Doyle LA, Ross DD. 2003. Multidrug resistance mediated by the breast cancer resistance protein BCRP (ABCG2). *Oncogene* 22:7340–7358. <https://doi.org/10.1038/sj.onc.1206938>.
- Konig J, Nies AT, Cui YH, Leier I, Keppler D. 1999. Conjugate export pumps of the multidrug resistance protein (MRP) family: localization, substrate specificity, and MRP2-mediated drug resistance. *Biochim Biophys Acta Biomembr* 1461:377–394. [https://doi.org/10.1016/S0005-2736\(99\)00169-8](https://doi.org/10.1016/S0005-2736(99)00169-8).
- Chan LM, Lowes S, Hirst BH. 2004. The ABCs of drug transport in intestine and liver: efflux proteins limiting drug absorption and bioavailability. *Eur J Pharm Sci* 21:25–51. <https://doi.org/10.1016/j.ejps.2003.07.003>.
- Lee G, Dallas S, Hong M, Bendayan R. 2001. Drug transporters in the central nervous system: brain barriers and brain parenchyma considerations. *Pharmacol Rev* 53:569–596. <https://doi.org/10.1146/annurev.pharmtox.41.1.569>.
- Lee W, Kim RB. 2004. Transporters and renal drug elimination. *Annu Rev Pharmacol Toxicol* 44:137–166. <https://doi.org/10.1146/annurev.pharmtox.44.101802.121856>.
- Bart J, Hollema H, Groen HJ, de Vries EG, Hendrikse NH, Sleijfer DT, Wegman TD, Vaalburg W, van der Graaf WT. 2004. The distribution of drug-efflux pumps, P-gp, BCRP, MRP1 and MRP2, in the normal blood-testis barrier and in primary testicular tumours. *Eur J Cancer* 40:2064–2070. <https://doi.org/10.1016/j.ejca.2004.05.010>.
- Koepsell H, Lips K, Volk C. 2007. Polyspecific organic cation transporters: structure, function, physiological roles, and biopharmaceutical implications. *Pharm Res* 24:1227–1251. <https://doi.org/10.1007/s11095-007-9254-z>.
- Gorboulev V, Ulzheimer JC, Akhoundova A, Ulzheimer-Teuber I, Karbach U, Quester S, Baumann C, Lang F, Busch AE, Koepsell H. 1997. Cloning and characterization of two human polyspecific organic cation transporters. *DNA Cell Biol* 16:871–881. <https://doi.org/10.1089/dna.1997.16.871>.
- Motohashi H, Sakurai Y, Saito H, Masuda S, Urakami Y, Goto M, Fukatsu A, Ogawa O, Inui K. 2002. Gene expression levels and immunolocaliza-

- tion of organic ion transporters in the human kidney. *J Am Soc Nephrol* 13:866–874.
21. Motohashi H, Inui K. 2013. Organic cation transporter OCTs (SLC22) and MATEs (SLC47) in the human kidney. *AAPS J* 15:581–588. <https://doi.org/10.1208/s12248-013-9465-7>.
 22. FDA. 2012. Guidance for industry, drug interaction studies—study design, data analysis, implications for dosing, and labeling recommendations. *Clinical Pharmacology*. FDA, Silver Spring, MD.
 23. Zamek-Gliszczynski MJ, Hoffmaster KA, Tweedie DJ, Giacomini KM, Hillgren KM. 2012. Highlights from the International Transporter Consortium Second Workshop. *Clin Pharmacol Ther* 92:553–556. <https://doi.org/10.1038/clpt.2012.126>.
 24. Giacomini KM, Huang SM, Tweedie DJ, Benet LZ, Brouwer KL, Chu X, Dahlin A, Evers R, Fischer V, Hillgren KM, Hoffmaster KA, Ishikawa T, Keppler D, Kim RB, Lee CA, Niemi M, Polli JW, Sugiyama Y, Swaan PW, Ware JA, Wright SH, Yee SW, Zamek-Gliszczynski MJ, Zhang L. 2010. Membrane transporters in drug development. *Nat Rev Drug Discov* 9:215–236. <https://doi.org/10.1038/nrd3028>.
 25. Zhang L, Zhang YD, Zhao P, Huang SM. 2009. Predicting drug-drug interactions: an FDA perspective. *AAPS J* 11:300–306. <https://doi.org/10.1208/s12248-009-9106-3>.
 26. EMA. 2012. Guideline on the investigation of drug interactions. *European Medicines Agency*, London, United Kingdom.
 27. Weiss J, Haefeli WE. 2013. Potential of the novel antiretroviral drug rilpivirine to modulate the expression and function of drug transporters and drug-metabolising enzymes in vitro. *Int J Antimicrob Agents* 41:484–487. <https://doi.org/10.1016/j.ijantimicag.2013.01.004>.
 28. Moss DM, Liptrott NJ, Curley P, Siccardi M, Back DJ, Owen A. 2013. Rilpivirine inhibits drug transporters ABCB1, SLC22A1, and SLC22A2 in vitro. *Antimicrob Agents Chemother* 57:5612–5618. <https://doi.org/10.1128/AAC.01421-13>.
 29. Cohen CJ, Molina JM, Cassetti I, Chetchotisakd P, Lazzarin A, Orkin C, Rhame F, Stellbrink HJ, Li T, Crauwels H, Rimsky L, Vanveggel S, Williams P, Boven K, ECHO, THRIVE Study Groups. 2013. Week 96 efficacy and safety of rilpivirine in treatment-naïve, HIV-1 patients in two phase III randomized trials. *AIDS* 27:939–950. <https://doi.org/10.1097/QAD.0b013e32835cee6e>.
 30. Curran A, Rojas J, Cabello A, Troya J, Imaz A, Domingo P, Martinez E, Ryan P, Gorgolas M, Podzamczar D, Knobel H, Gutierrez F, Ribera E. 2016. Effectiveness and safety of an abacavir/lamivudine + rilpivirine regimen for the treatment of HIV-1 infection in naïve patients. *J Antimicrob Chemother* 71:3510–3514. <https://doi.org/10.1093/jac/dkw347>.
 31. Palacios R, Perez-Hernandez IA, Martinez MA, Mayorga ML, Gonzalez-Domenech CM, Omar M, Olalla J, Romero A, Romero JM, Perez-Camacho I, Hernandez-Quero J, Santos J. 2016. Efficacy and safety of switching to abacavir/lamivudine (ABC/3TC) plus rilpivirine (RPV) in virologically suppressed HIV-infected patients on HAART. *Eur J Clin Microbiol Infect Dis* 35:815–819. <https://doi.org/10.1007/s10096-016-2602-3>.
 32. Troya J, Ryan P, Ribera E, Podzamczar D, Hontanon V, Terron JA, Boix V, Moreno S, Barrufet P, Castano M, Carrero A, Galindo MJ, Suarez-Lozano I, Knobel H, Raffo M, Solis J, Yllescas M, Esteban H, Gonzalez-Garcia J, Berenguer J, Imaz A, GESIDA-8314 Study Group. 2016. Abacavir/lamivudine plus rilpivirine is an effective and safe strategy for HIV-1 suppressed patients: 48 week results of the SIMRIKI retrospective study. *PLoS One* 11:e0164455. <https://doi.org/10.1371/journal.pone.0164455>.
 33. Ceckova M, Reznicek J, Ptackova Z, Cerveny L, Muller F, Kacerovsky M, Fromm MF, Glazier JD, Staud F. 2016. Role of ABC and solute carrier transporters in the placental transport of lamivudine. *Antimicrob Agents Chemother* 60:5563–5572. <https://doi.org/10.1128/AAC.00648-16>.
 34. Müller F, König J, Hoier E, Mandery K, Fromm MF. 2013. Role of organic cation transporter OCT2 and multidrug and toxin extrusion proteins MATE1 and MATE2-K for transport and drug interactions of the antiviral lamivudine. *Biochem Pharmacol* 86:808–815. <https://doi.org/10.1016/j.bcp.2013.07.008>.
 35. Cihalova D, Hofman J, Ceckova M, Staud F. 2013. Purvalanol A, olomoucine II and roscovitine inhibit ABCB1 transporter and synergistically potentiate cytotoxic effects of daunorubicin in vitro. *PLoS One* 8:e83467. <https://doi.org/10.1371/journal.pone.0083467>.
 36. Ceckova M, Libra A, Pavek P, Nachtigal P, Rabec M, Fuchs R, Staud F. 2006. Expression and functional activity of breast cancer resistance protein (BCRP, ABCG2) transporter in the human choriocarcinoma cell line bewo. *Clin Exp Pharmacol Physiol* 33:58–65. <https://doi.org/10.1111/j.1440-1681.2006.04324.x>.
 37. Zhang L, Zhang YD, Strong JM, Reynolds KS, Huang SM. 2008. A regulatory viewpoint on transporter-based drug interactions. *Xenobiotica* 38:709–724. <https://doi.org/10.1080/00498250802017715>.
 38. Taipalensuu J, Tornblom H, Lindberg G, Einarsson C, Sjoqvist F, Melhus H, Garberg P, Sjoström B, Lundgren B, Artursson P. 2001. Correlation of gene expression of ten drug efflux proteins of the ATP-binding cassette transporter family in normal human jejunum and in human intestinal epithelial Caco-2 cell monolayers. *J Pharmacol Exp Ther* 299:164–170.
 39. Brown KC, Paul S, Kashuba AD. 2009. Drug interactions with new and investigational antiretrovirals. *Clin Pharmacokinet* 48:211–241. <https://doi.org/10.2165/00003088-200948040-00001>.
 40. Han HK. 2011. Role of transporters in drug interactions. *Arch Pharm Res* 34:1865–1877. <https://doi.org/10.1007/s12272-011-1107-y>.
 41. König J, Müller F, Fromm MF. 2013. Transporters and drug-drug interactions: important determinants of drug disposition and effects. *Pharmacol Rev* 65:944–966. <https://doi.org/10.1124/pr.113.007518>.
 42. Müller F, Fromm MF. 2011. Transporter-mediated drug-drug interactions. *Pharmacogenomics* 12:1017–1037.
 43. Langmann T, Mauerer R, Zahn A, Moehle C, Probst M, Stremmel W, Schmitz G. 2003. Real-time reverse transcription-PCR expression profiling of the complete human ATP-binding cassette transporter superfamily in various tissues. *Clin Chem* 49:230–238.
 44. Shapiro AB, Ling V. 1998. The mechanism of ATP-dependent multidrug transport by P-glycoprotein. *Acta Physiol Scand* 163:227–234.
 45. Mittra R, Pavy M, Subramanian N, George AM, O'Mara ML, Kerr ID, Callaghan R. 2016. Location of contact residues in pharmacologically distinct drug binding sites on P-glycoprotein. *Biochem Pharmacol* <https://doi.org/10.1016/j.bcp.2016.10.002>.
 46. Garvey L, Winston A. 2009. Rilpivirine: a novel non-nucleoside reverse transcriptase inhibitor. *Expert Opin Investig Drugs* 18:1035–1041. <https://doi.org/10.1517/13543780903055056>.
 47. Sharma M, Saravolatz LD. 2013. Rilpivirine: a new non-nucleoside reverse transcriptase inhibitor. *J Antimicrob Chemother* 68:250–256. <https://doi.org/10.1093/jac/dks404>.
 48. Crauwels H, van Heeswijk RPG, Stevens M, Buelens A, Vanveggel S, Boven K, Hoetelmans R. 2013. Clinical perspective on drug-drug interactions with the non-nucleoside reverse transcriptase inhibitor rilpivirine. *AIDS Rev* 15:87–101.
 49. National Research Council. 1996. *Guide for the care and use of laboratory animals*. National Academies Press, Washington, DC. <http://www.ncbi.nlm.nih.gov/books/NBK54050>.
 50. Council of Europe. 1986. *European convention for the protection of vertebrate animals used for experimental and other scientific purposes*. European treaty series no. 123. Council of Europe, Strasbourg, France.
 51. Tong L, Phan TK, Robinson KL, Babusis D, Strab R, Bhoopathy S, Hidalgo IJ, Rhodes GR, Ray AS. 2007. Effects of human immunodeficiency virus protease inhibitors on the intestinal absorption of tenofovir disoproxil fumarate in vitro. *Antimicrob Agents Chemother* 51:3498–3504. <https://doi.org/10.1128/AAC.00671-07>.